

---

# Influence of Restoration Type on Stress Distribution in Bone Around Implants: A Three-Dimensional Finite Element Analysis

Roxana Stegaroiu, DDS\*/Takahiro Sato, DDS, PhD\*\*/Haruka Kusakari, DDS, PhD\*\*\*/  
Osamu Miyakawa, BE, DDSc\*\*\*\*

---

The three-dimensional finite element analysis method was used to assess stress in bone around titanium implants using three treatment designs for a partially edentulous mandible, under axial (AX), buccolingual (BL), or mesiodistal (MD) loads. For each of these loads, highest stress was calculated in the model with a cantilever prosthesis supported by two implants (M2). Less stress was found in the model with a conventional fixed partial denture on two implants (M3), and lowest stress was calculated in the model with three connected crowns supported by three implants (M1). When BL load was applied to M3, cortical bone stress was high, comparable to that calculated for M2 under the same load. When AX or MD load was applied to M3, the cortical bone stress was low, similar to that found in M1 under each of these loads.

(INT J ORAL MAXILLOFAC IMPLANTS 1998;13:82-90)

**Key words:** bone stress, dental implants, fixed partial prosthesis, three-dimensional finite element analysis

---

Clinical studies have reported high success rates in partially edentulous patients treated with implant-supported fixed partial prostheses<sup>1-5</sup>; however, they also have reported variable rates of failure. Implant failure is reported to be caused by poor oral hygiene,<sup>6-8</sup> biomechanical factors,<sup>6,7,9-12</sup> poor bone

quality,<sup>1,3,13</sup> and medical status of the patient.<sup>14,15</sup> To reduce failure rates, appropriate management of these factors is required.

The importance of biomechanical factors has been stressed by various authors.<sup>16-18</sup> The biologic response of bone to mechanical loads affects implant longevity.<sup>12</sup> Animal experiments and clinical studies have shown that, in the absence of plaque-related gingivitis, bone loss around implants is associated with unfavorable loading conditions.<sup>5,6,19-21</sup> Since load is transferred to bone through prosthesis and implant, careful planning and execution of the prosthesis is an important factor in achieving appropriate stress distribution in the bone.<sup>18</sup>

Recently, stress distribution in bone correlated with implant-supported prosthesis design has been investigated mainly by means of two-dimensional (2D) and three-dimensional (3D) finite element analyses (FEAs). Studies comparing the accuracy of these analyses found that, if detailed stress information is required, then 3D modeling will be necessary.<sup>22</sup> Results of 3D FEA were compared with in

---

\*Postgraduate Student, Department of Fixed Prosthodontics, School of Dentistry, Niigata University, Niigata, Japan.

\*\*Instructor, Department of Fixed Prosthodontics, School of Dentistry, Niigata University, Niigata, Japan.

\*\*\*Professor and Chairman, Department of Fixed Prosthodontics, School of Dentistry, Niigata University, Niigata, Japan.

\*\*\*\*Professor and Chairman, Department of Dental Materials and Technology, School of Dentistry, Niigata University, Niigata, Japan.

**Reprint requests:** Dr Roxana Stegaroiu, Department of Fixed Prosthodontics, School of Dentistry, Niigata University, Gakkocho-Dori 2-5274, Niigata 951, Japan. E-mail: roxana@dent.niigata-u.ac.jp

vivo strain-gauge measurements<sup>23</sup> and with in vitro experimental setups.<sup>22</sup> In both studies, the results of the 3D FEA matched the experimental measurements in tendency. The 3D FEA is considered an appropriate method for investigation of the stress throughout a three-dimensional structure, and it was selected for bone stress evaluation in this study.

Marginal bone resorption was reported<sup>6</sup> and predicted<sup>24,25</sup> for implant-supported full-arch prostheses with long cantilever arms. Marginal bone loss was correlated with the high bone stress calculated for the cantilever full-arch prostheses.<sup>16,23,25,26</sup> Several 3D FEAs investigated bone stress around implants supporting full-arch prostheses.<sup>23,26-29</sup> In contrast, only a few 3D FEAs were performed on models with fixed partial prostheses supported by implants.<sup>30,31</sup> In these studies, models of fixed prostheses in which two missing teeth were replaced in the posterior mandible were employed to analyze the effect of tooth-to-implant connection on bone stress. In clinical practice, three-unit prostheses with or without cantilever extensions and supported by free-standing implants are also used in partially edentulous mandibles. However, no 3D FEA bone stress analyses were reported for these prosthesis designs.

In this study, a 3D FEA was conducted to compare the stress distribution in a mandibular posterior segment restored with different types of three-unit prostheses and supported by free-standing implants.

## Materials and Methods

**Model Design.** A mandibular segment with implants and superstructure was modeled on a personal computer (PC-H98, NEC, Tokyo, Japan), using a finite element program (Ansys 5.0, Swanson Analysis System, Houston, PA). The number of implants and type of superstructure varied according to the model, as follows:

- Model 1: Three implants supporting three connected crowns (M1) (Fig 1a)
- Model 2: Two implants supporting a cantilever prosthesis (M2) (Fig 1b)
- Model 3: Two implants supporting a conventional fixed partial denture (M3) (Fig 1c)

The bone was modeled as a cancellous core surrounded by a 2-mm-thick cortical layer, except in the upper part, where the cortical layer was flattened to obtain 1 mm of thickness (Figs 2a and 2b). For implant longevity, it is important to maintain at least 1 mm of bone buccally and lingually at the implant neck.<sup>32</sup> In this study, bone plates of at least 1.16 mm in width were modeled in those regions.

Titanium implants and abutments were modeled using a 16.5-mm-long, 4-mm diameter cylinder. Thirteen millimeters of this cylinder corresponded to the implant, 10 mm of which were buried in the bone. These dimensions approximate those of the 10-mm-length bone-anchorage implant and the 3.5-mm-high abutment from the ITI system, but the geometry of both components was simplified to that of a cylinder. A gold framework and a 1.5-mm-thick porcelain veneer were applied over the titanium abutments, so as to obtain a prosthesis measuring 8 mm in width and 6 mm in height (Figs 2a and 2b). A simplified shape of the crowns was modeled. Identical geometry of the superstructure was used in all models to allow for comparison of the results (Figs 1a to 1c).

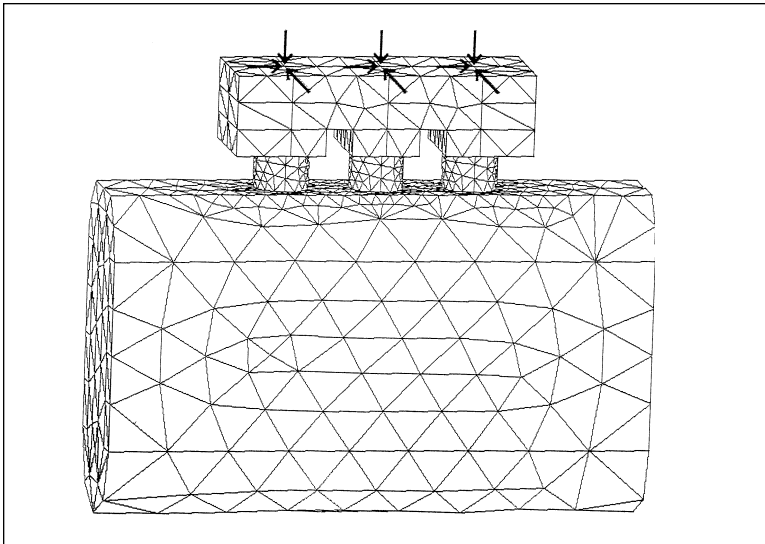
**Material Properties.** All materials used in the models were considered to be isotropic, homogeneous, and linearly elastic. The elastic properties used were taken from the literature (Table 1).

**Interface Condition.** To simulate ideal osseointegration, the implants, along their entire interface, were rigidly anchored in the bone model. The same type of contact was provided at all material interfaces.

**Elements and Nodes.** Models were meshed with four-node tetrahedron elements. A finer mesh was generated at the material interfaces to ensure accuracy of force transfer. Mesh around the implant neck is illustrated in Fig 3. The number of elements and nodes in each model is as follows: 14,773 elements and 2,954 nodes in M1; 10,774 elements and 2,251 nodes in M2; and 10,685 elements and 2,237 nodes in M3.

**Constraints and Loads.** Models were constrained in all directions at the nodes on the inferior border of the bone surface, on one fifth of the bone height. Direction and magnitude of the maximum occlusal force show large variations.<sup>36</sup> However, any force can be resolved into three components along convenient axes, and the effect of each component can be individually assessed.<sup>11,16</sup> In linearly elastic materials, the effect of any force can be simply computed if the effect of the unit force is known. Therefore, unit-static loads (1 N) were applied to the occlusal key point in the center of each prosthetic unit (Figs 1a to 1c). The models were separately analyzed for the axial (AX), buccolingual (BL), and mesiodistal (MD) load sets.

**Solution.** Analysis for each loading condition was performed by means of the Ansys software program, which was run on a personal computer with a pentium 133 MHz central processing unit. The calculation time was about 3 hours for each model. The von Mises stress<sup>26</sup> (equivalent stress, here abbreviated EQV) was used to display the stress in the bone.



**Figs 1a to 1c** Three-dimensional finite element models of a mandibular segment (cortical and cancellous bone), implants, and fixed partial prostheses. Unit forces (1 N) were applied axially, buccolingually, and mesiodistally, sequentially, to the center of each prosthetic unit.

**Fig 1a** Three connected crowns on three implants (M1).

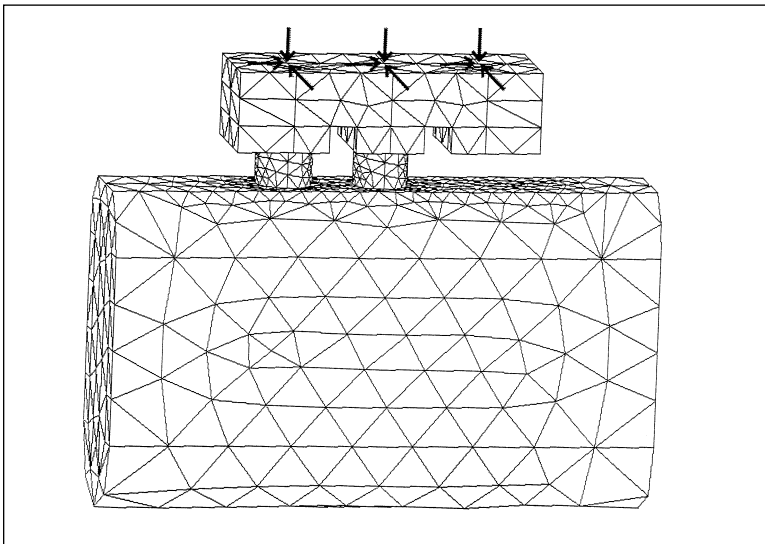


**Fig 1b** Cantilever prosthesis on two implants (M2).

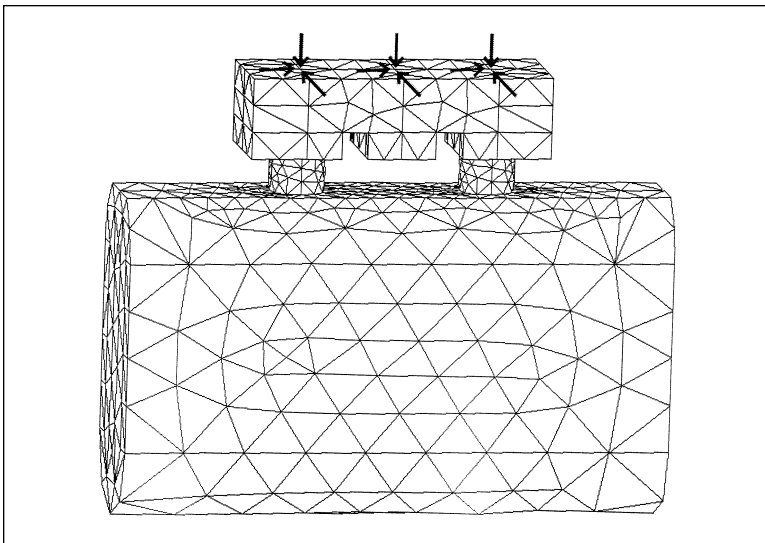
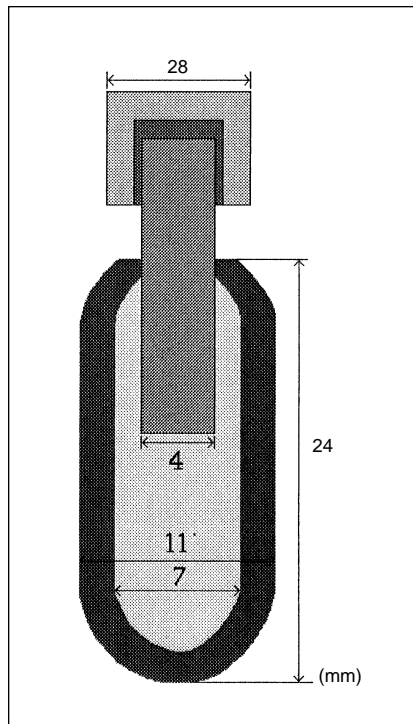
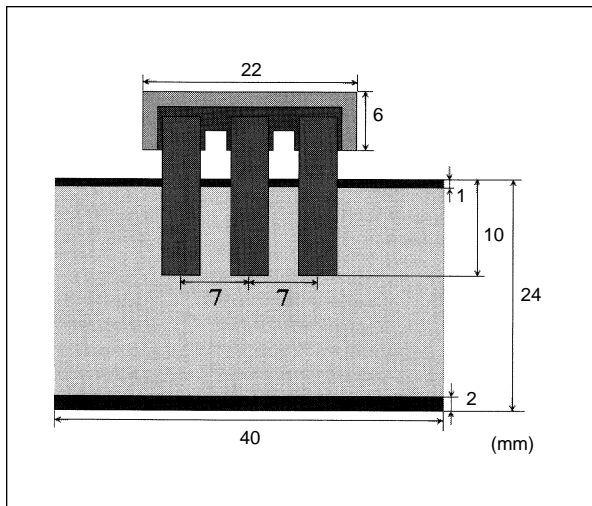


**Fig 1c** Conventional fixed partial denture on two implants (M3).

**Table 1** Elastic Properties Ascribed to Materials Used in the Models

Material	Young's modulus (GPa)	Poisson's ratio
Cortical bone <sup>33</sup>	15	0.3
Cancellous bone <sup>33</sup>	1.5	0.3
Titanium <sup>33,34</sup>	110	0.35
Gold alloy <sup>26</sup>	90	0.3
Porcelain* <sup>35</sup>	70	0.22

\*For porcelain, elastic properties of glass were used.



**Figs 2a and 2b** Mesiodistal (*top*) and buccolingual (*right*) sections of M1. Three implants placed in a cancellous bone core surrounded by cortical bone are supporting a fixed partial prosthesis (black = gold framework; gray = porcelain veneer).

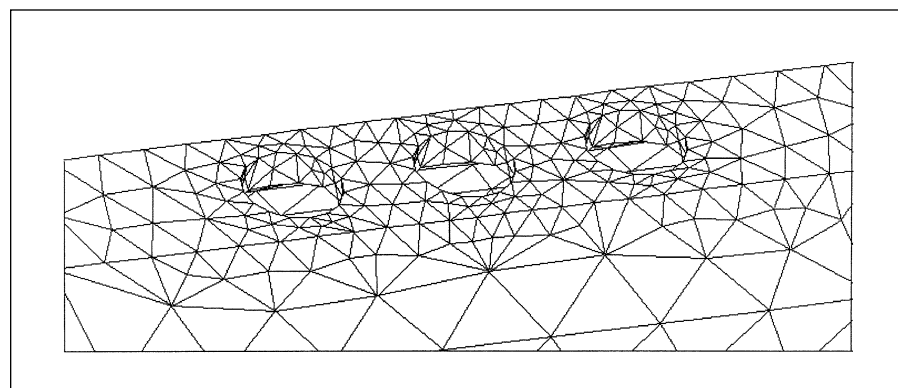
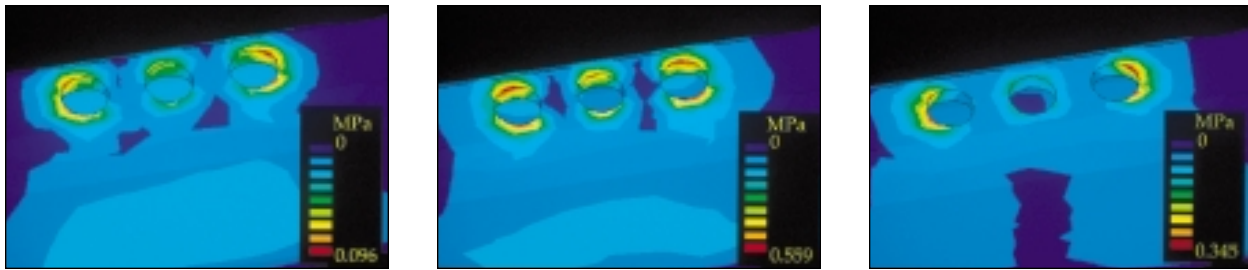
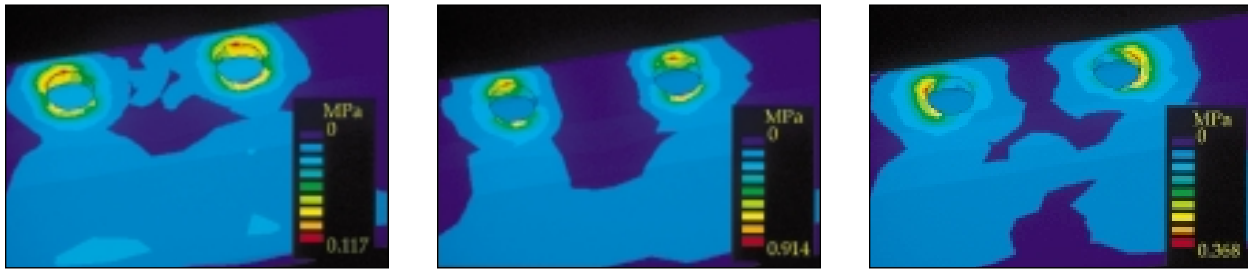


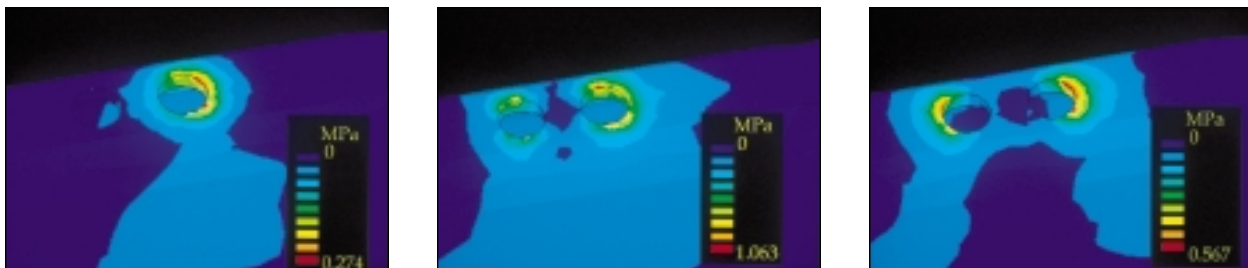
**Fig 3** Close-up view of the meshed cortical bone in M1 (cancellous bone and implants are not shown).



**Figs 4a to 4c** Close-up view of the equivalent stress distribution in cortical bone in M1: (left) under axial loads; (center) under buccolingual loads; and (right) under mesiodistal loads.



**Figs 5a to 5c** Close-up view of the equivalent stress distribution in cortical bone in M3: (left) under axial loads; (center) under buccolingual loads; and (right) under mesiodistal loads.



**Figs 6a to 6c** Close-up view of the equivalent stress distribution in cortical bone in M2: (left) under axial loads; (center) under buccolingual loads; and (right) under mesiodistal loads.

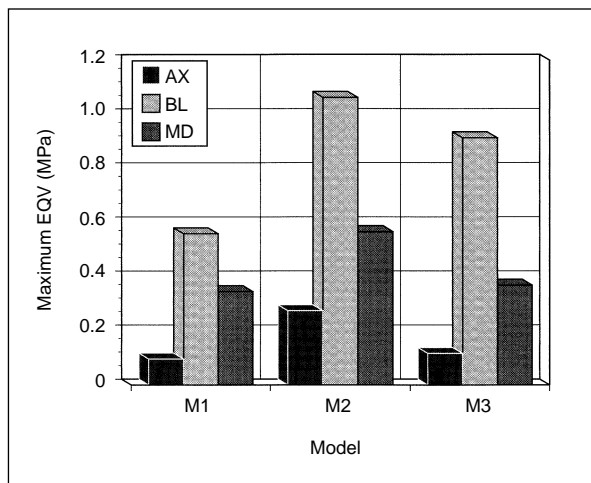


**Fig 7** Maximum equivalent stress in cortical bone, in all the models, under axial (AX), buccolingual (BL), and mesiodistal loads (MD).

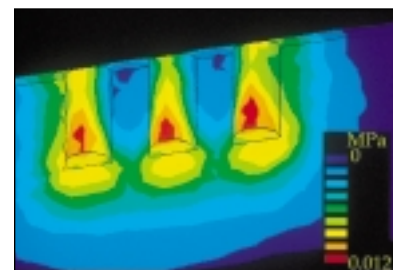


**Fig 8** Close-up view of the equivalent stress distribution in cancellous bone (mesiodistal section) in M1, under axial loads.

## Results

Stress distribution in the cortical bone is exhibited using different scales, enabling comprehensive display of stress concentration in each case. Regardless of model and load direction, highest stress was concentrated around the implant neck.

In both M1 and M3, the EQV distribution in the bone was orthogonally symmetric (Figs 4a to 4c and 5a to 5c).

In both M1 and M3, AX loads acted along the longitudinal axis of the implant and perpendicular to the long axis of the bone. They caused bone compression at the implant bottom and shear stress at the lateral interface of the implants. Prosthesis and implants were displaced in the vertical plane.

In both M1 and M3, BL loads perpendicular to the long axes of the bone and the implant caused tilting of the prosthesis and implants towards the lingual, yielding compressive and tensile stresses in the cortical bone around implants, on the lingual and buccal sides, respectively.

In both M1 and M3, MD loads parallel to the longitudinal axis of the bone and perpendicular to the implant axis caused a rotation of the prosthesis and implants in the vertical plane, yielding compressive and tensile stress in the cortical bone distally to the distal implant and mesially to the mesial implant, respectively.

In M2, stress was mainly concentrated around the distal implant under AX and BL loads (Figs 6a and 6b). Under AX loads, the cantilever pontic tended to rotate the prosthesis in the vertical plane. Under BL loads, in addition to the tilting towards the lingual, a rotation in the horizontal plane occurred as an effect

of the load applied to the cantilever pontic. Under MD loads, displacement type and stress distribution were similar to those in M1 and M3, but the values were different (Fig 6c).

Maximum EQV in the cortical bone for all investigated models is shown in Fig 7. This graph enables comparison of the maximum EQV in the same model for different loading conditions and among different models for the same loading condition. In all models, stress was highest under BL loads and lowest under AX loads. Maximum EQV in the cortical bone decreased in the following order: M2, M3, and M1. The ratio between M1:M2:M3 was 1:2.9:1.2 under the AX loads; 1:1.9:1.6 under the BL loads; and 1:1.6:1.1 under the MD loads. Under BL loads, stress in M3 was high, comparable to that in M2 and much higher than that in M1; but under AX and MD loads, stress in M3 was low, similar to that in M1.

Stress distribution in the cancellous bone is shown in Fig 8. Under AX loads, highest stress was concentrated apically, especially in the buccal and lingual bone plates. However, under BL and MD loads, highest stress was calculated in the neck region.

Maximum EQV in the cancellous bone for all investigated models is displayed in Fig 9. The ratio between maximum EQV for M1:M2:M3 was 1:2.2:1.2 under the AX loads; 1:1.8:1.2 under the BL loads; and 1:1.6:1.0 under the MD loads. The stress values reached only about one tenth or less of the corresponding values in the cortical bone. Despite this quantitative difference, qualitative similarity is evident (Figs 7 and 9).

## Discussion

This study used the 3D FEA method to compare the stress distribution in a mandibular posterior segment with implants supporting three different types of fixed prostheses (M1, M2, M3). Result accuracy of a 3D FEA relies on the precision of the simulation model. In a comparative analysis such as this, complex reality can be simplified assuming that proportions and relative effects accurately reflect reality.<sup>27</sup>

In this study, a segment of bone was modeled to simulate the posterior region of the mandible. Its size was chosen so that the end effects (stress extended to the ends of the bone segment) should not impinge on the results at the region of interest. Sato et al<sup>37</sup> reported, in a 3D FEA study, that variations in the bone stress around an implant were negligible if the length of bone between implant and segment end was at least 4.2 mm. Since, in the present study, this length was 11 mm, and even longer at the distal end in M2, the end effects were considered to be negligible and did not alter the results.

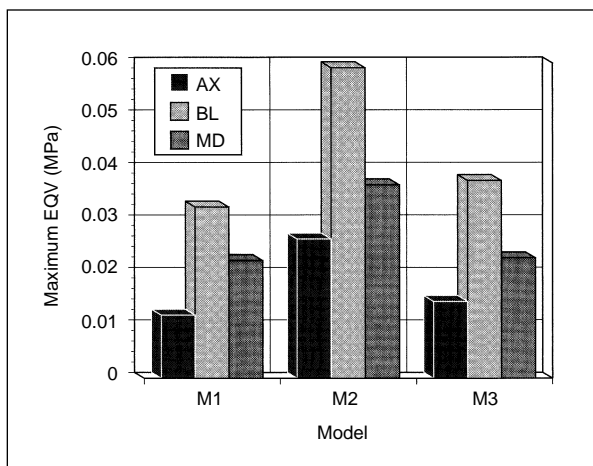


**Fig 9** Maximum equivalent stress in cancellous bone, in all the models, under axial (AX), buccolingual (BL), and mesio-distal (MD) loads.

Loads were applied to the occlusal surface of the superstructure, and constraints were applied to the inferior border of the bone. When loading and boundary conditions were set up, forces and reactions during occlusion were taken into consideration. Physiologically, occlusal forces are generated by the masticatory muscles, and they produce reactions at the temporomandibular joints and at the occlusal bite point, where the movement of the mandible is restrained.<sup>36</sup> These physiologic conditions could be approximated by simulating the whole mandibular body, but since that would be elaborate and time consuming, smaller models are proposed. Meijer et al<sup>27</sup> reported in a 3D FEA study that similar results were obtained when the entire mandible was modeled, with loading and boundary conditions approximating the physiologic ones and with simulation of only the interforaminal region.

In the present study, loads and restraints were simplified since only part of the mandible was modeled. Although this simplification could be expected to bring about quantitative changes in the results, it was not expected to influence them qualitatively. The location of loads (force) and restraints (reaction) was reversed from that of the real situation, but this reversal should not have significantly affected the results, since a force and its reaction have the same value.

Unit forces were used to calculate the stress in bone. Since all the materials in the models were linearly elastic, the stress increased proportionally with the load. It would be tempting to use the results of this study to deduce the maximum bone stress for physiologic loads for each prosthesis type; however, for the convenience of the analysis, material properties, loads, boundary, and interface conditions were simplified in the model. The bone was considered to be linearly elastic, homogeneous, and isotropic, and the implants were considered to be rigidly bound to the bone over their entire surface. Since the reality is more complex than this simulation,<sup>38-40</sup> a qualitative comparison among models is advisable rather than focusing on quantitative data from FEA.<sup>30</sup> The predictions of FEAs are reliable for the proportions between stress values.<sup>27</sup> Therefore, the results were reported as ratios between the maximum EQV in bone for the three prosthesis types, which allowed for comparison between the models.

The results of this analysis concur with findings of other studies that used different investigation methods; therefore, the model employed in this study is considered to satisfactorily simulate reality.

The tendency of stress concentration around the implant neck, which was evident in all of the models (Figs 4 to 6), is consistent with other results from FEA of loaded implants, as well as with findings from

in vitro and in vivo experiments and clinical studies, which demonstrated bone loss initiating around the implant neck.<sup>10,19,41-43</sup>

Under AX and MD loads, stress in M1 (Figs 4a and 4c) and M3 (Figs 5a and 5c) was higher in the cortical bone mesially to the mesial implant and distally to the distal implant than it was between implants. In M1, stress around the central implant was lower than that around the other implants. In linearly elastic materials, stress values correspond to the gradient of displacement, namely deformation. Because the implants were rigidly anchored into the bone and the bone volume between implants was rather small, the bone between implants, along with the implants, was almost uniformly displaced. Thus, this small bone deformation resulted in a low stress in the bone between implants. For the same reason, lower stress was found around the central implant in M1. In contrast, at the mesial part of the mesial implant and at the distal part of the distal implant, the surrounding bone volume was large, and it opposed a higher resistance to the action of the loads. Therefore, the bone close to the implants was more displaced than that located further away, and higher stress was concentrated near the implants.

Under AX and MD loads, bone around the central implant in M1 bore only a small amount of stress compared with bone around the other two implants (Figs 4a and 4c). Thus, the absence of the central implant in M3 did not strongly influence the maximum EQV, and similar values were found for M1 and M3 under AX and MD loads (Fig 7). However, under BL loads, bone around the central implant in M1 bore a degree of stress comparable to that around the other two implants (Fig 4b). Therefore, the absence of the central implant in M3 determined substantial augmentation of the maximum EQV compared to the value in M1 under BL loads (Fig 7).

In M2, the high stress around the distal half of the distal implant, which was found under AX loads, resulted from both the rotation in the vertical plane and the load applied to that implant. The rotation acted so as to extract the mesial implant, but this action was canceled by the AX load applied to that implant. Thus, almost no stress was found around the mesial implant (Fig 6a). Under BL loads, the deformations that occurred as a combined effect of the rotations in the transversal and horizontal planes yielded increased stress around the distal implant and lower stress around the mesial implant (Fig 6b).

As predicted by Skalak,<sup>16</sup> bone stress was higher under lateral loads than under axial loads. The rotation induced by the BL and MD loads was responsible for the higher values of the maximum EQV under these loads (Fig 7). In all the models, higher bone

stress was calculated under the BL loads than under MD loads. This was the result of the larger gradient of bone displacement under BL loads than under MD loads. In light of the high stress calculated for BL forces in each model, when planning and fabricating a superstructure it is important to create an occlusal shape that minimizes lateral force components. The same principle should be considered during the occlusal adjustment.

This study used a 1:1:1 ratio for AX, BL, and MD loads, respectively. However, intraorally, axial components of occlusal forces are much larger than the buccolingual and mesiodistal ones. For example, a ratio of 5:2.5:1 was found during chewing by Graf<sup>44</sup> and by Graf et al.<sup>45</sup> Therefore, the ratios among stress induced by AX, BL, and MD loads in each model will differ proportionally from those calculated for unit loads. Because axial force components are larger than lateral ones, stress induced by axial loads may also challenge the bone. This applies especially for the cantilever model, where, in this study, the stress caused by the axial loads was more than twice as great as the corresponding stress in the other models.

The high stress calculated in M2 is in accordance with the results reported for full-arch cantilever prostheses under one-point loading,<sup>16,23,25,26</sup> and may represent a risk for the bone-implant interface.

The stress values and distribution in M3 may suggest that in occlusions with predominant axial force components, a conventional fixed partial denture supported by two implants could be an alternative treatment, if anatomic or financial reasons limit the placement of three implants. However, in occlusions with large buccolingual force components, a conventional fixed partial denture would induce high bone stress, comparable to that from a cantilever prosthesis.

The present study focused on the influence of prosthesis type (a main feature of prosthesis design) on bone stress. The shape of implant and superstructure was simplified to reduce the factors that could impinge on the results. A more refined geometry of the model, various interface conditions, and different prosthesis materials are factors that could possibly influence bone stress.

## Conclusions

A cantilever implant prosthesis (M2) may induce high bone stress, while connected crowns supported by three implants (M1) may induce low bone stress. Furthermore, under three-point load with predominant axial components, a conventional fixed partial denture supported by two implants (M3) may create bone stress comparable to that calculated for connected crowns supported by three implants (M1).

However, in occlusions with large buccolingual force components, only the connected crowns supported by three implants may minimize the harmful effect of these loads.

## References

1. Lekholm U, van Steenberghe D, Hermann I, Bolender C, Folmer T, Gunne J, et al. Osseointegrated implants in the treatment of partially edentulous jaws: A prospective 5-year multicenter study. *Int J Oral Maxillofac Implants* 1994;9:627-635.
2. van Steenberghe D, Sullivan D, Liström R, Balshi T, Henry PJ, Worthington P, et al. A retrospective multicenter evaluation of the survival rate of osseointegrated fixtures supporting bridges in the treatment of partial edentulism. *J Prosthet Dent* 1989;61:217-223.
3. Buser D, Weber H-P, Brägger U, Balsiger C. Tissue integration of one-stage implants: Three-year results of a prospective longitudinal study with hollow cylinder and hollow screw implants. *Quintessence Int* 1994;25:679-686.
4. Laney W, Jemt T, Harris D, Henry P, Krogh P, Polizzi G. Osseointegrated implants for single-tooth replacement: Progress report from a multicenter prospective study after 3 years. *Int J Oral Maxillofac Implants* 1994;9:49-54.
5. Naert I, Quirynen M, van Steenberghe D, Darius P. A six-year prosthodontic study of 509 consecutively inserted implants for the treatment of partial edentulism. *J Prosthet Dent* 1992;67:236-245.
6. Lindquist LW, Rockler B, Carlsson E. Bone resorption around fixtures in edentulous patients treated with mandibular fixed tissue-integrated prostheses. *J Prosthet Dent* 1988;59:59-63.
7. Payant L, Williams JE, Zwemer JD. Survey of dental implant practice. *J Oral Implantol* 1994;20:50-58.
8. Lindhe J, Berglundh T, Ericsson I, Liljeborg B, Marinello C. Experimental breakdown of peri-implant and periodontal tissues: A study in the beagle dog. *Clin Oral Implants Res* 1992;3:9-16.
9. Brånemark P-I. Osseointegration and its experimental background. *J Prosthet Dent* 1983;50:399-410.
10. Adell R, Lekholm U, Rockler B, Brånemark P-I. A 15-year study of osseointegrated implants in the treatment of the edentulous jaw. *Int J Oral Surg* 1981;10:387-416.
11. Brunski JB. Biomechanical factors affecting the bone-dental implant interface. *Clin Mater* 1992;10:153-201.
12. Warren Bidez M, Misch C. Issues in bone mechanics related to oral implants. *Implant Dent* 1992;1:289-294.
13. LeGeros RZ, Craig RG. Strategies to affect bone remodeling: Osteointegration. *J Bone Miner Res* 1993;8:583-596.
14. Weyant RJ. Characteristics associated with the loss and peri-implant tissue health of endosseous dental implants. *Int J Oral Maxillofac Implants* 1994;9:95-102.
15. Weyant RJ, Burt BA. An assessment of survival rates and within-patient clustering of failures for endosseous oral implants. *J Dent Res* 1993;72:2-8.
16. Skalak R. Aspects of biomechanical considerations. In: Brånemark P-I, Zarb GA, Albrektsson T (eds). *Tissue-Integrated Prostheses: Osseointegration in Clinical Dentistry*. Chicago: Quintessence, 1985:117-128.
17. Carter DR, Spengler DM. Mechanical properties and composition of cortical bone. *Clin Orthop* 1977;127:265-274.
18. Brånemark P-I, Hansson BO, Adell R, Breine U, Lindström J, Hallen O, et al. Osseointegrated implants in the treatment of the edentulous jaw: Experience from a 10-year period. *Scand J Plast Reconstr Surg* 1977;11 (suppl 16):1-132.



19. Hoshaw SJ, Brunski JB, Cochran GVB. Mechanical loading of Brånemark implants affects interfacial bone modeling and remodeling. *Int J Oral Maxillofac Implants* 1994;9:345-360.
20. Quirynen M, Naert I, van Steenberghe D. Fixture design and overload influence marginal bone loss and fixture success in the Brånemark system. *Clin Oral Implants Res* 1992;3:104-111.
21. Naert I, Quirynen M, van Steenberghe D, Darius P. A study of 589 consecutive implants supporting complete fixed prostheses. Part II: Prosthetic aspects. *J Prosthet Dent* 1992;68:949-956.
22. Simon BR, Woo SL-Y, Stanley GM, Olmstead SR, McCarty MP, Jemmott GF, et al. Evaluation of one-, two-, and three-dimensional finite element and experimental models of internal fixation plates. *J Biomech* 1977;10:79-86.
23. Benzing UR, Gall H, Weber H. Biomechanical aspects of two different implant-prosthetic concepts for edentulous maxillae. *Int J Maxillofac Implants* 1995;10:188-198.
24. Adell R. Long term treatment results. In: Brånemark P-I, Zarb GA, Albrektsson T. (eds). *Tissue-Integrated Prostheses: Osseointegration in Clinical Dentistry*. Chicago: Quintessence, 1985:175-186.
25. Warren Bidez M, Misch CE. Force transfer in implant dentistry: Basic concepts and principles. *J Oral Implantol* 1992;18:264-274.
26. van Zyl PP, Grundling NL, Jooste CH, Terblanche E. Three-dimensional finite element model of a human mandible incorporating six osseointegrated implants for stress analysis of mandibular cantilever prostheses. *Int J Oral Maxillofac Implants* 1995;10:51-57.
27. Meijer HJA, Starmans FJM, Bosman F, Steen WHA. A comparison of three finite element models of an edentulous mandible provided with implants. *J Oral Rehabil* 1993;20:147-157.
28. Meijer HJA, Starmans FJM, Steen WHA, Bosman F. Location of implants in the interforaminal region of the mandible and the consequences for the design of the superstructure. *J Oral Rehabil* 1994;21:47-56.
29. Davis DM, Zarb GA, Chao Y-L. Studies on frameworks for osseointegrated prostheses: Part 1. The effect of varying the number of supporting abutments. *Int J Oral Maxillofac Implants* 1988;3:197-201.
30. Misch CM, Ismail YH. Finite element stress analysis of tooth-to-implant fixed partial denture designs. *J Prosthodont* 1993;2:83-92.
31. Sato T, Kusakari H, Miyakawa O. Three dimensional finite element analysis of bone around dental implants in posterior mandibular region: Biomechanics of implant connections. *J Jpn Prosthodont Soc* 1996;40:682-694.
32. Buser D, Maeglin B. Chirurgisches Vorgehen mit ITI-Implantaten. In: Schroeder A, Sutter F, Buser D, Krekeler G (eds). *Orale Implantologie: Allgemeine Grundlagen und ITI-System*. Stuttgart: Georg Thieme Verlag, 1994:260-328.
33. van Rossen IP, Braak LH, de Putter C, de Groot K. Stress-absorbing elements in dental implants. *J Prosthet Dent* 1990;64:198-205.
34. Steinemann S. Werkstoff Titan. In: Schroeder A, Sutter F, Buser D, Krekeler G (eds). *Orale Implantologie: Allgemeine Grundlagen und ITI-System*. Stuttgart: Georg Thieme Verlag, 1994:37-59.
35. Tokyo Astronomical Observatory. *Chronological Scientific Tables* (in Japanese: Rika Nenpyo). Tokyo: Maruzen, 1985:438.
36. Koolstra JH, van Eijden TMGJ, Weijs WA, Naeije M. A three-dimensional mathematical model of the human masticatory system predicting maximum possible bite forces. *J Biomech* 1988;21:563-576.
37. Sato Y, Teixeira ER, Shindoi N, Wadamoto M, Akagawa Y. Effect of bone length on stress distribution in implant FEA [abstract]. *J Dent Res* 1997;76:328.
38. Carter DR, Spengler DM. Mechanical properties and composition of cortical bone. *Clin Orthop* 1978;135:192-264.
39. McElhaney JH, Fogle JL, Melvin JW, Haynes RR, Roberts VL, Alem NM. Mechanical properties of cranial bone. *J Biomech* 1970;3:495-511.
40. Carr AB, Gerard DA, Larsen PE. Characterization of bone supporting three different biomaterials in baboon jaws [abstract]. *J Dent Res* 1997;76:24.
41. Clelland NL, Gilat A, McGlumphy EA, Brantley WA. A photoelastic and strain gauge analysis of angled abutments for an implant system. *Int J Oral Maxillofac Implants* 1993;8:541-548.
42. Lozada JL, Abbate MF, Pizzarello FA, James RA. Comparative three-dimensional analysis of two finite-element endosseous implant designs. *J Oral Implantol* 1994;20:315-321.
43. Morgan MJ, James DF, Pilliar RM. Fractures of the fixture component of an osseointegrated implant. *Int J Oral Maxillofac Implants* 1993;8:409-414.
44. Graf H. Bruxism. *Dent Clin North Am* 1969;13:659-665.
45. Graf H, Grassel H, Aeberhard HJ. A method for the measurement of occlusal forces in three directions. *Helv Odont Acta* 1974;18:7-11.